Computer Simulation of Physical Systems: Report

Antonino Emanuele Scurria

December 2022

1 Introduction

In this report we are interested in analyzing the results obtained simulating a Lennard-Jones fluid through different tecniques: the first one will be a NVE simulation performed through Molecular Dynamics; the second one a NVT simulation through Molecular dynamics and Nosé-Hoover thermostat; the third one will be a Monte Carlo NVT simulation. In order to compare the different approaches we will focus on some particular physical quantities: the correlation function, the structure factor and finally the diffusion coefficient.

2 NVE Simulation

The aim of this section is to recreate the simulation of Rahman's study of an NVE simulation exploiting Molecular Dynamics algorithms. The physical system we are going to simulate is made up of $N = 864$ atoms of liquid Argon at $T = 94.4°K$ and a density of $\rho = 1.374\,\mathrm{gcm}^{-3}$ (the single atomic mass $M = 6.69 * 10^{-23}g$). The physical structure will be a face-centered cubic lattice made up of 6 cells for each axis (so that we have 4 particles for each cell) and we consider periodic boundary conditions. Moreover the lattice spacing parameter of the face-centered cubic cell is = 1.7048 in LJ units. During our simulation we consider a time step = $0.0046ps$ in order to have a similar time step of the one used in Rahman's simulation ($10^{-14}s$). Finally we consider a L.J potential 1 as interaction between the different particles and a cutoff radius = 2.5 using LJ units (it corresponds to $8.5\mathring{A}$)

$$V(r) = 4\varepsilon\left[\left(\frac{\sigma}{r}\right)^{12} - \left(\frac{\sigma}{r}\right)^{6}\right] \tag{1}$$

with $\sigma = 3.4\mathring{A}$ and $\varepsilon/k_B = 120$ K.

2.1 Initial Setup

The first step of the simulation is to generate the FCC lattice: for this purpose we exploit a function called $'crystal'$ that generates the particles of each cell with setting the initial positions and velocities: positions of the 4 different particles of each cell are set to $(0,0,0)$ $(1/2,1/2,0)$ $(1/2,0,1/2)$ and $(0,1/2,1/2)$ in the unit cell; velocities' projections on each axes are generated according to a normal distribution of parameter $\mu = 0$ and $\sigma = \sqrt{T}$ where $T = 0.7867$ (Maxwell-Boltzmann distribution of velocities with $T = 94.4°K$). After this initial step we run a simulation (function $'run\_NVE'$) of the dynamics including a rescaling of the velocities in order to set the temperature of the system to the one desired (in this case $T = 94.4°K$, so that we can compare our results to Rahman's results; it is also important to underline that in this case we are not running a simulation in the NVE ensemble since we are changing the total energy of the system; moreover we are not running a simulation in the NVT ensemble, for which we will use the Nosé-Hoover thermostat and the MCMC approaches, since only in the thermodynamic limit we observe vanishing oscillations of the temperature around its mean). After this step we run a simulation in the NVE ensemble starting from the configuration of the previous run to

equilibrate the system (the value of the energy is now stable) and we can start to measure the properties we want to analyze.

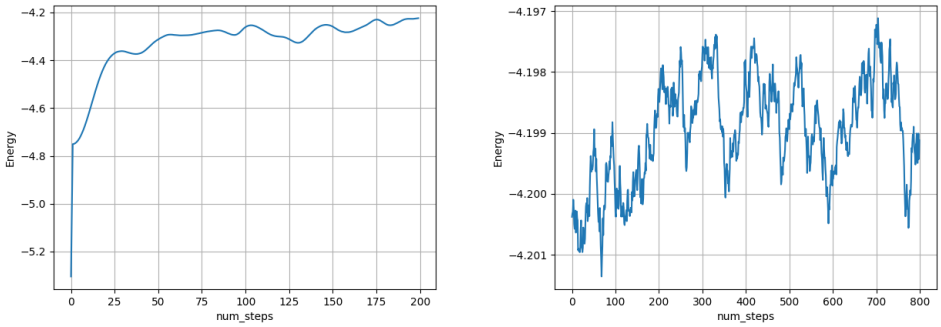

Figure 1: Energy (per particle) of the system in the first run (left), in which we can observe a drift , and the second run to equilibrate the system (right).

2.2 Static Properties

The first quantity we want to measure, after we brought the system at equilibrium, is the correlation function: :

$$g(r) = \frac{1}{\rho_0} \sum_{j=1}^{N} \delta\left(r - r_{ij}\right) \qquad r_{ij} = |\vec{r}_i - \vec{r}_j| \tag{2}$$

($\rho_0 = (N-1)/V$where V is the total volume and N is the number of particles). After calculating the correlation function we exploit the Fourier transform to calculate the structure factor S :

$$S(Q) = 1 + 4\pi\rho_0 \int_0^\infty r^2 (g(r) - 1) \frac{\sin Qr}{Qr} dr. \tag{3}$$

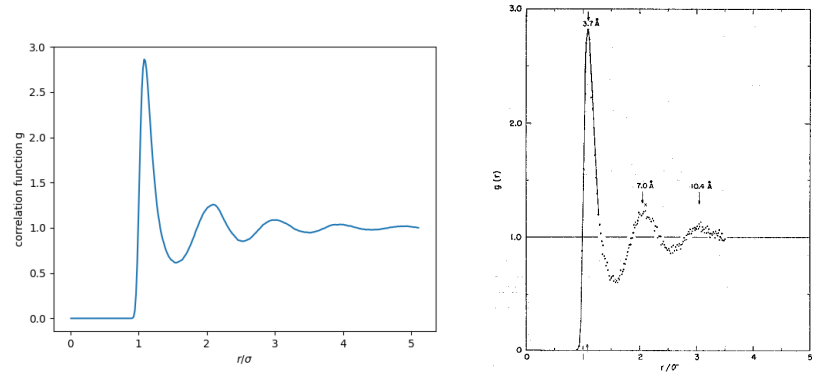

Figure 2: Radial pair correlation function of the system obtained by our simulation (left) and Rahman simulation (right).

As we can see by the plots 2 and 3 and the respective tables, we get results very similar to the ones achieved by Rahman. Moreover it is also interesting to observe how these observed quantities behave varying the parameters we are taking into account for this simulation: the temperature, the density and the cutoff radius. Performing several numerical experiments we obtained the following results: looking at the the plots 4 we can

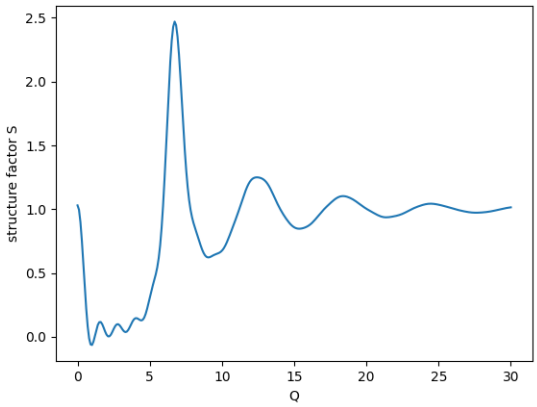

Figure 3: Plot of and $S(Q)$.

Peaks	$r[\mathring{A}]$	
	Simulation	Rahman
First Peak	3.68	3.7
Second Peak	7.05	7.0
Third Peak	10.19	10.4

Table 1: Coordinates of the observed peaks of $g(r)$.

Peaks	$Q/\sigma[1/\mathring{A}]$		
	Simulation	Rahman	X-rays
First Peak	$1,97$	2.0	2.0
Second Peak	3.66	3.68	3.61
Third Peak	5.41	5.41	5.41
Fourth Peak	7.20	7.29	7.17

Table 2: Coordinates of the observed peaks of $S(Q)$.

observe that we get a significant difference for the two quantities only with $r\_cutoff = 1$: thus we understand that particles that are more than 1.5 (L.J. units) distant don't influence the computation of the two quantities and this is due to the form of the potential we are taking into account (L.J. potential).

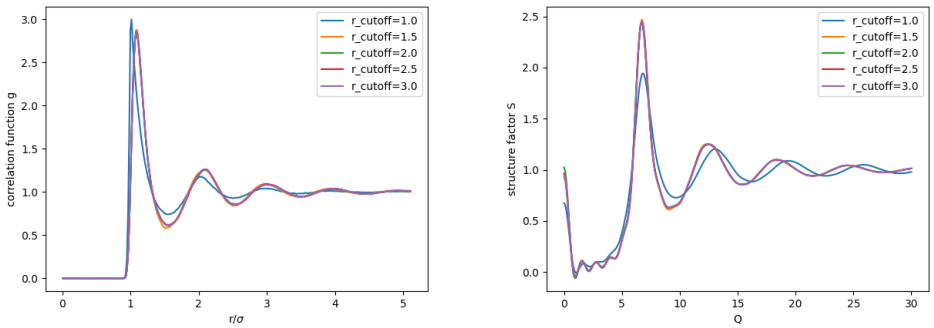

Figure 4: Plot of the correlation function (left) and the structure factor (right) with different cutoff radii.

Moreover observing plots 5 we notice that we don't get significant differences in the position of the peaks (even though there are small differences in the peaks' values).

Finally, looking at plots 6 we observe that the position of the peaks are weakly shifted while we have small differences in the value of the amplitude. In the latter case it is also important to notice that using the last density we observe many oscillations in the structure factor and this is due to expression we are using for calculating S, that is 3: we are facing numerical instabilities due to the integrand ; we could avoid this by exploiting the direct calculation of S but it would take a lot of computational resources and, in this case, it would take several hours.

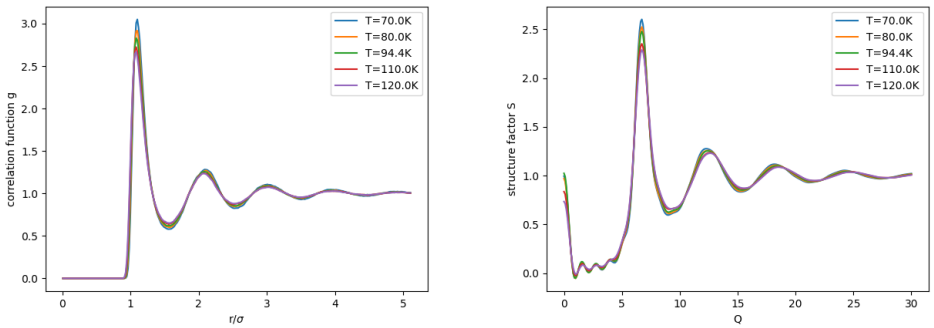

Figure 5: Plots of the correlation function (left) and the structure factor (right) at different temperatures.

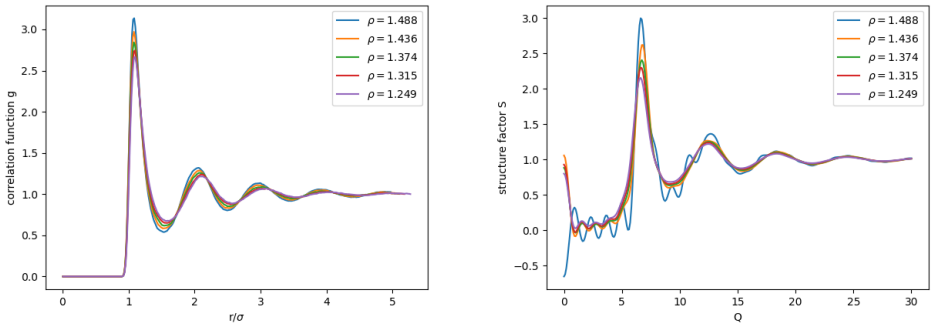

Figure 6: Plots of the correlation function (left) and the structure factor (right) at different densities.

2.3 Dynamic Properties

In this section we are now interested in obtaining the diffusion coefficient D of our system: we will use 2 different approaches that are based on two different formulas. The fist way to obtain D is through the velocity autocorrelation function 4 and the equivalence shown in 5. The second way of obtaining D is based on the Einstein relation 6 for the diffusion coefficient. As we can see, ideally, we have to consider an infinite time to achieve these 2 equalities: for this reason in the first case we will pay attention to capture all the major contribution of 5 in order to neglect only very small contribution in the total integral; in the second case we will pay attention to the behaviour of the Mean Squared Displacement: indeed we will look for a linear regime of the MSD to obtain a reasonable value of the diffusion coefficient (since the limit of 6 is equal to a constant we aim to find something

in the linear regime in the t variable)

$$\mathcal{VACF}(\tau) = \frac{\langle \vec{v}(\tau) \cdot \vec{v}(0) \rangle}{\langle \vec{v}(0) \cdot \vec{v}(0) \rangle} \tag{4}$$

$$D = \int_0^\infty d\tau < V_x(\tau) V_x(0) > \tag{5}$$

$$D = \lim_{t \to \infty} \frac{1}{6t} \left\langle \|\Delta \vec{r}(t)\|^2 \right\rangle \cong \frac{1}{6t} \frac{1}{N} \sum_{i=1}^{N} \|\vec{r}_i\,(t + t_0) - \vec{r}_i\,(t_0)\|^2 \tag{6}$$

2.3.1 Numerical results

To compute the diffusion coefficient D we use the previous formulas 12 different runs and then we calculate the mean curve of all the previous obtained.

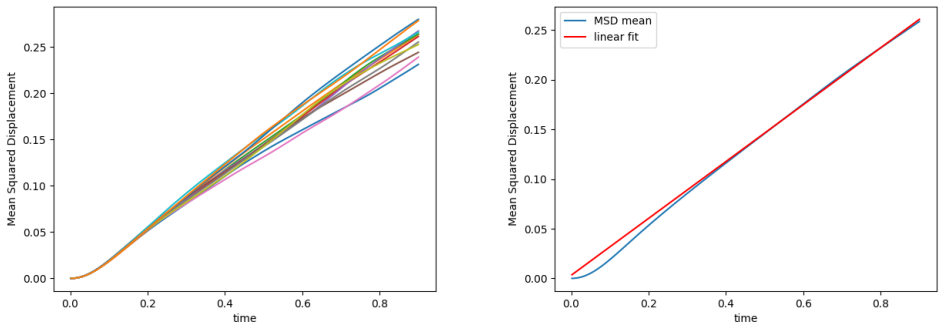

Figure 7: Plots of all the MSDs obtained in the different runs (left) and the mean of them (right). Here we are using L.J. units.

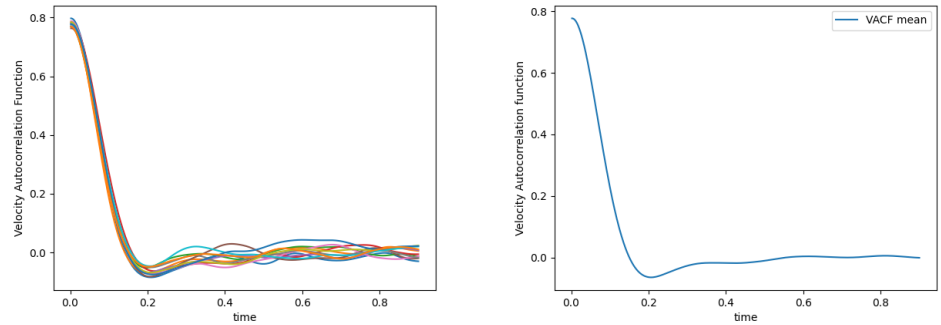

Figure 8: Plots of all the VACFs obtained in the different runs (left) and the mean of them (right). Here we are using L.J. units.

Method	Diffusion Coefficient $[cm^2/s]$
MSD	$(2.415 \pm 0.15) * 10^{-5}$
VACF	$(2.450 \pm 0.13) * 10^{-5}$
Rahman	$2.43 * 10^{-5}$

As we can see form the plots of the various quantities both in the first and second case we are able to overcome the infinite time problem: in the plot of the MSD we observe, indeed, that we achieve a linear regime within the time of our simulation. For the second case, with VACF, we observe that we manage to obtain all the meaningful contribution to the integral within the time of our simulation.

3 NVT Simulation with Nosé-Hoover thermostat

In this section we are going to analyze the results obtained with a NVT simulation performed through the Nosé-Hoover thermostat: we are going to augment our Hamiltoninan with some fictitious variables in order to perform molecular dynamics that will give us the correct averages in the canonical ensemble. The Lagrangian of the augmented system reads as follows:

$$\mathcal{L}_{\text{Nosé}}\ (\{r_i\}, \{\dot{r}_i\}, s, \dot{s}) = \sum_{i=1}^{N} 1/2 m_i s^2 \dot{r}_i^2 - U\left(r^N\right) + 1/2 Q \dot{s}^2 - \frac{g}{\beta} \ln s$$

Now, imposing $g = 3*N+1$, where N is the number of particles and choosing Q arbitrarily we can perform an NVE MD simulation with respect to the correspondent Hamiltonian and this will give us correct values for the canonical ensemble average. It is important to underline that the value of Q will affect the velocity of the fluctuations of the temperature we observe during the simulation: using a large Q will 'slow down' the fluctuations whereas using a small Q will cause the opposite effect. Another important feature of the choice of Q lies in the fact that if we choose such a value that the fluctuations of the temperature have a larger period (usually 10x) than the vibrational fluctuations of the particles we can also obtain some meaningful insights into the dynamic of the system: in practice, what we usually do, in order to reduce the duration of the simulation, is to avoid the previous procedure and to consider that , since Q is related to only a degree of freedom, the choice of the period will not dramatically affect the dynamics of the system.

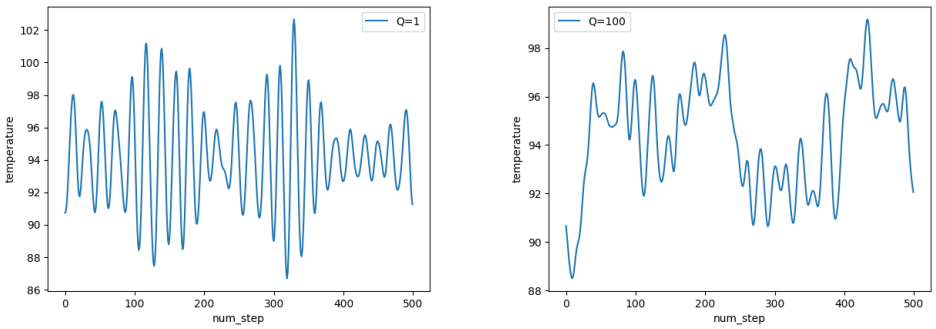

Figure 9: Plots of the temperature with respect to the correspondent step during the NVT simulation. As we can see we use two different values of Q: on the left we set $Q = 1(KJ/mol)(ps)^2$ whereas on the right we use $Q = 1(KJ/mol)(ps)^2$. In these two figures we can see that the choice of Q influences the period of the fluctuations of the temperature around the value of $T = 94.4°K$ as previously said.

3.1 Numerical Results

At first we run a simulation to equilibrate the system with a temperature of $T = 94.4°K$. The time step of the simulation is the same of the NVE simulation performed before.

After we equilibrate the system we aim to analyze the distribution of the velocities that should be equal to the Maxwell-Boltzmann distribution to ensure the correctness of our results (see 11). Another important test we can perform is to check that the construction of the augmented system doesn't depend on the choice of Q since, as previously said, it can be chosen arbitrarily even though it affects the simulation (as previously observed). Figure 12 shows that the distribution of velocities doesn't depend on the value of Q.

We now want to compute the pair correlation function and the structure factor (see 13): we obtain results perfectly equal (with the precision we are using) to the previous results obtained with the NVE ensemble. Then we compute the diffusion coefficient through

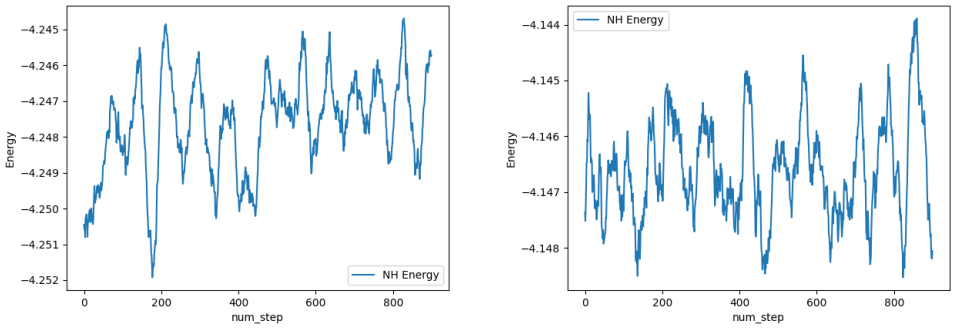

Figure 10: Plots of the Nosé-Hoover Hamiltonian with respect to the correspondent step during the the simulation to equilibrate (left) and a later simulation. As we can see the first simulation shows a weak drift in the total energy of the augmented system and for this reason we need to perform a first simulation to obtain an equilibrium configuration before measuring the quantities we want to analyze (it is important to underline that in the first simulation we set the augmented variables to 0 by default, whereas in later simulations we use the value obtained by the very previous run).

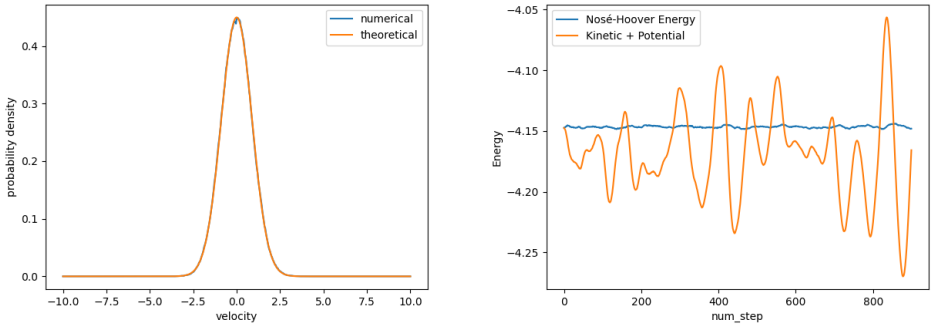

Figure 11: Plot of velocity distribution of the simulation (left). As we can see the numerical results perfectly match the theoretical prevision. On the right we compare the fluctuations of the 'real' energy and the energy of the augmented system.

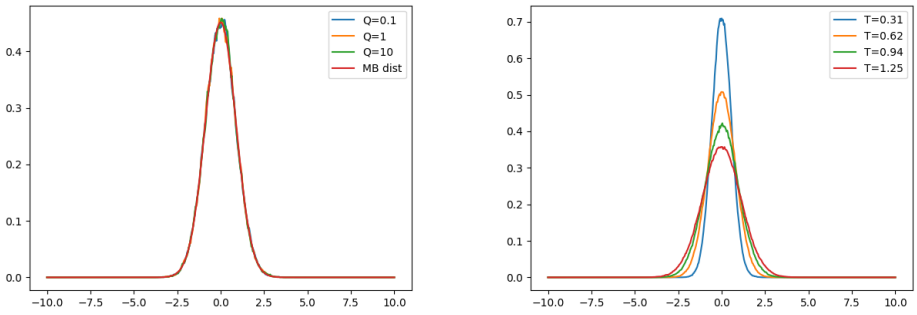

Figure 12: Plot of velocity distribution for different values of Q (left) $[(KJ/mol)(ps)^2]$. On the right we have the plot of different distribution of velocities for different values of the temperature: as we can see all the distribution behave like a Maxwell-Boltzmann distribution whose width depends on the temperature.

the Einstein relation used in the previous NVE simulation: it is important to underline that the simulation in the NVT ensemble through the Nosé-Hoover Hamiltonian doesn't allow us to compute dynamic quantities since we are dealing with an augmented dynamics and not a real dynamics. Nonetheless, even without a proper theoretical basis, we can compute the diffusion coefficient through the MSD and compare it with the previous simulation.

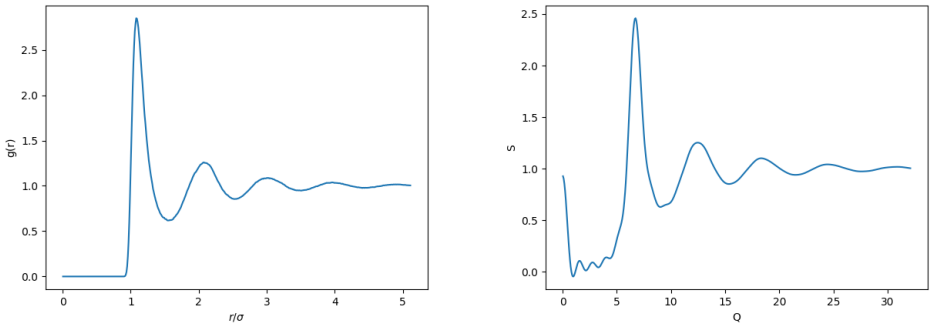

Figure 13: Plot of the pair correlation function (left) and the structure factor (right) obtained during NVT simulations with the Nosé-Hoover Hamiltonian.

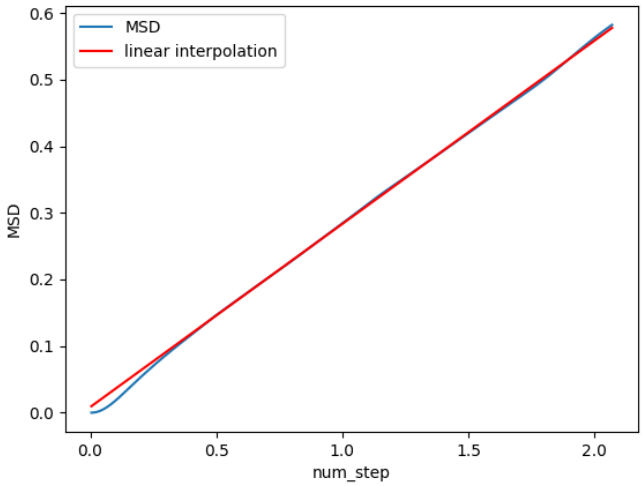

Figure 14: Plot of the MSD obtained through the NVT simulation. As we can observe the result is similiar to the one obtained through the VACF and the Einstein relation in the NVE simulation.

Method	Diffusion Coefficient $[cm^2/s]$
MSD	$(2.415 \pm 0.15) * 10^{-5}$
VACF	$(2.450 \pm 0.13) * 10^{-5}$
NVT MSD	$(2.452 \pm 0.33) * 10^{-5}$
Rahman	$2.43 * 10^{-5}$

4 NVT with Monte Carlo Markov Chain

In this section we are going to analyze the simulation of the NVT ensemble through Monte Carlo (ergodic) Markov Chain method: this method is used to compute ensemble

averages (i.e. integrals) of different observables. The procedure consists in sampling new configurations of our system (i.e. points in the phase space) and accepting the new configuration sampled according to an algorithm (in this case we will use Metropolis-Hastings algorithm). The algorithm is chosen in order to ensure that the equilibrium probability distribution of our Markov Chain will be equal to our goal probability density: the canonical probability density. As previously said we are going to consider only the NVT ensemble since the NVE ensemble is better simulated with the standard MD procedure we presented before.

4.1 Initial Setup

In the simulations we are going to perform we use periodic boundary conditions. We will use two different lattice structures as initialization: the first is a simple cubic lattice of 200 particles at temperature $T = 2$ and density $\rho = 0.5$ in L.J. units and it will be used to study some properties of the Monte Carlo simulation (we always take into account a L.J. potential); the second structure is the same of the simulations of liquid Argon previously performed with MD techniques. The new configurations throughout the simulation are generated with a simple procedure that, experimentally, has been found to work optimally: each new configuration is generated choosing a random particle in the system and moving it up to a maximum distance *dmax* in each of the three directions (the new position is chosen according to a uniform distribution in each direction). Moreover each cycle of our simulation will be made up of 50 attempted displacements (50 new configurations). Finally , before calculating observables' averages, we perform an equilibration cycle to ensure the achievement of the equilibrium distribution.

4.2 First simulation

Here we are using the first described (in the previous sub-section) setting. At first we run an equilibration cycle and then we look at the energy and the pressure of the simulation to observe their behaviour. During the equilibration cycles we also adjust the maximum displacement *dmax* for each new configuration in order to get an acceptance rate of 50% that is more efficient. As we can see by 15 we immediately manage to obtain stable fluctuations around a mean value, both for the energy and the pressures. Moreover, it is important to underline that, in order to reduce the correlation between following samples of our observables, we impose a sampling frequency equal to 10 (we sample our observables every 10 cycles).

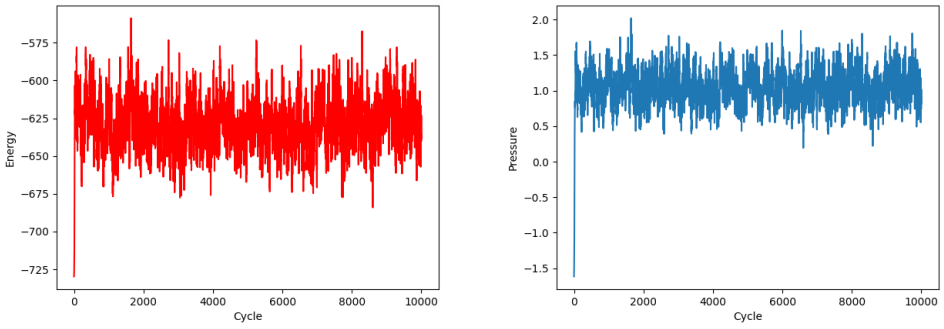

Figure 15: Evolution of the energy and the pressure for the first 10000 cycles of the simulations starting from a simple cubic lattice configuration.

Then we perform a blocking analysis to obtain the correlation time of our simulation using 50000 cycles: as we can see from 22, if we use only 50000 cycles we aren't able to localize the plateau region and the correlation time. For this reason we performed several simulations with a different number of cycles and we obtained a much better confidence

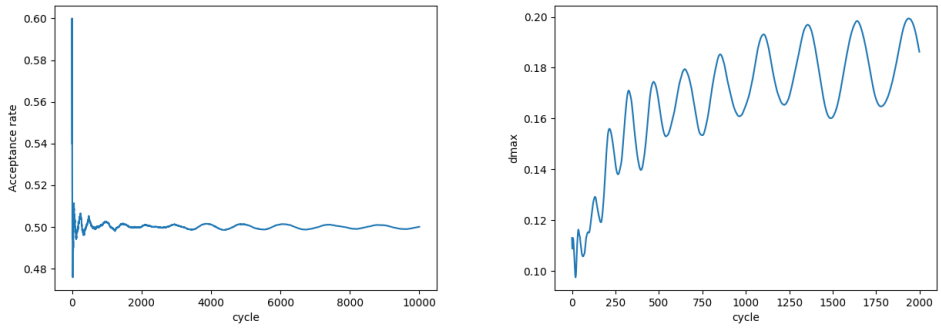

Figure 16: Plot of the evolution during the equilibration simulation of the acceptance rate and the maximum displacement per trial configuration $dmax$.

for localizing the plateau region with 3 000 000 cycles (the simulation takes a lot of time). Thus we can affirm, from 18 that the correlation time is approximately between 2^7 and 2^8. Moreover, always from 18, we observe that $\sigma_E = (2.62 \pm 0.07) * 10^{-4}$ and $\sigma_P = (7.35 \pm 0.15) * 10^{-4}$. It is interesting to observe how the uncertainty of the expected standard deviaton increases when we increase the increase the size of the blocks: this is due to the fact that we are exploiting the low of large numbers and therefor increasing the size we are decreasing the number of blocks and we obtain a worse convergence (recall that in the law of large numbers the standard deviation decreases as $1/\sqrt{N}$ where N is the number of samples).

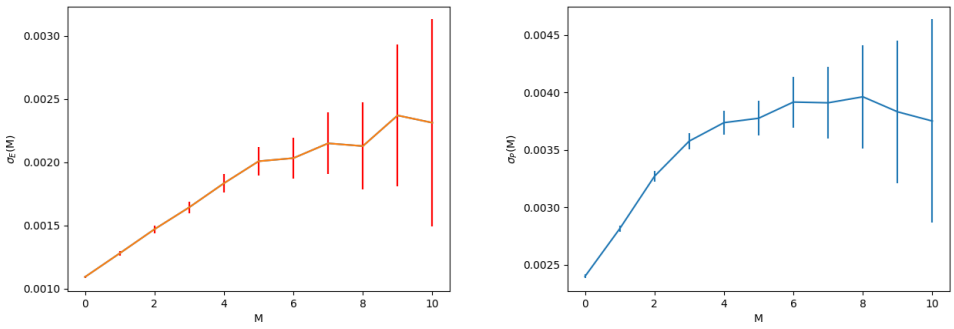

Figure 17: Plot of the standard deviation for the pressure (left) and the energy (right) considering 50 000: as we can observe we are not able to detect the plateau region with a high confidence. The vertical bars indicate the uncertainty of the expected value.

Then we calculate the isotherm at 2 different temperatures ($T = 240°K$ and $T = 108°K$, the latter is below the critical temperature) and we compare them with the same isotherms computed in Frenkel-Smit book. As we can see by figures 19 and 20 our simulation well matches with the simulation performed by Frenkel and Smit and the negative pressure we obtain is due a to transition phase (we are taking into account a temperature that is below the critical temperature).

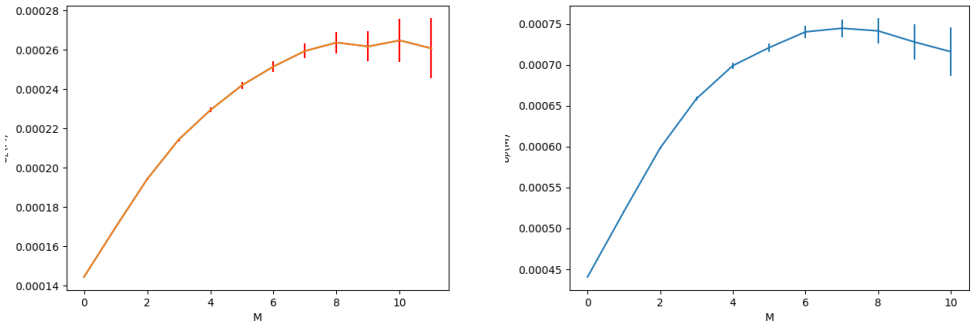

Figure 18: Plot of the standard deviation for the pressure (left) and the energy (right) considering 3 000 000 cycles to have a better confidence on the plateau region.The vertical bars indicate the uncertainty of the expected value.

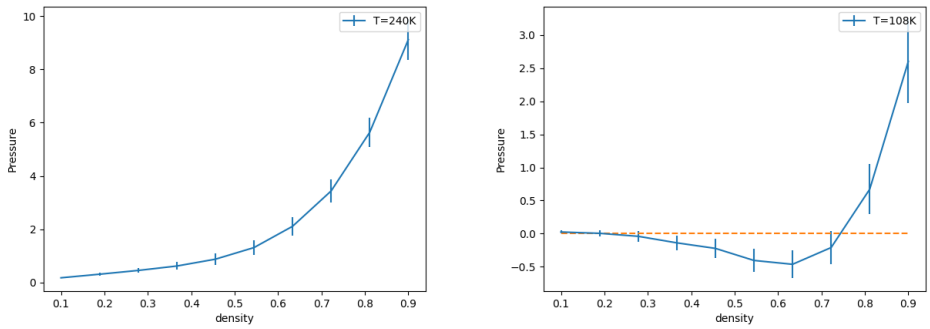

Figure 19: Plot of isotherm at $T = 2$ in L.J. units (left) and isotherm at $T = 0.9$ in L.J. (below the critical temperature) units (right). The vertical lines indicate the uncertainty (calculated through standard deviation) on the computed expected value (computed through sample mean). We are using L.J. units.

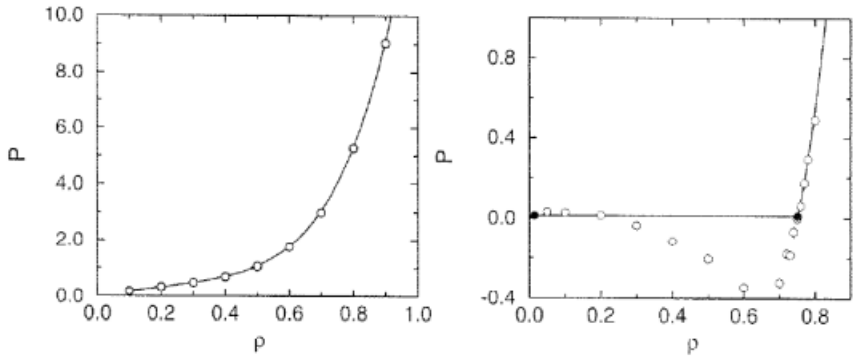

Figure 20: Plot from Frenkel-Smit book of isotherm at $T = 2$ in L.J. units (left) and isotherm at $T = 0.9$ in L.J. (below the critical temperature) units (right). The circles represent tha value obtained during the simulation while the solid curve on the left represents the theoretical curve. On the horizontal line is the saturated vapor pressure and the filled circles indicate the densities of coexisting vapor and liquid phases. We are using L.J. units.

4.3 Argon Simulation

In this section we are going to analyze the results of the simulation of liquid Argon with the same setting used for the 2 previous simulations. The MC simulation setting is equal to the setting used for the previous MD simulations of liquid Argon. The quantities we are going to analyze are the pair correlation function and the structure factor. As described in section 4.2 first we are going to perform an equilibration cycle and then we are going to compute the ensemble averages of our observables. At first we repeat very same procedure of the previous section to study how many cycles do we need to equilibrate our system and eventually we choose a value of 10 000 cycles (in this case the convergence of the energy and, mostly, of the pressure is slower than in the previous case). Then we perform a blocking analysis to obtain the correlation time in order to set the sampling frequency. Now we can compute $g(r)$ and $S(Q)$ and we get similar results to the previous simulations

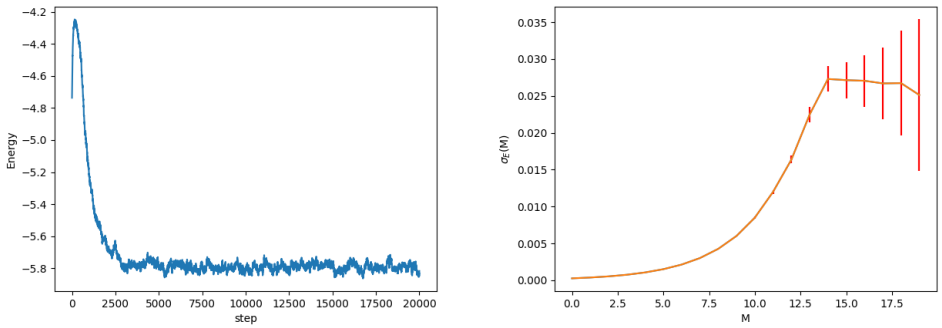

Figure 21: Plot of Energy per particle (in L.J. units) during the first simulations (left) and blocking analysis (right).

in the NVE and NVT ensembles performed through MD algorithms, as we can see by the tables 4.3 and 4.3.

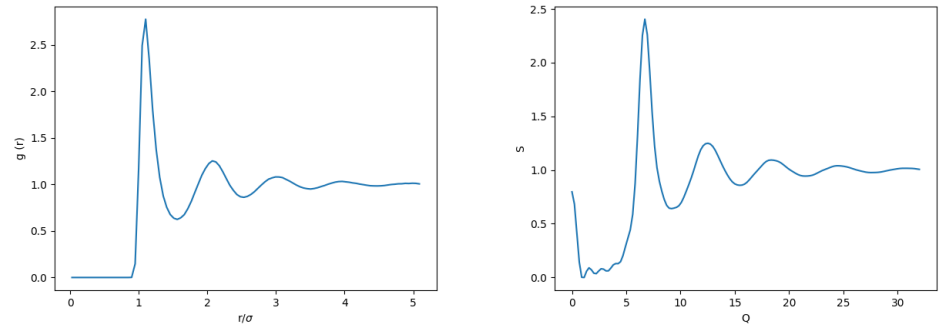

Figure 22: Plot of the pair correlation function and the structure factor obtained during the MCMC simulation.

Peaks	$r[\AA]$		
	NVE/N-H NVT Simulation	MCMC Simulation	Rahman
First Peak	3.68	3.72	3.7
Second Peak	7.05	7.12	7.0
Third Peak	10.19	10.25	10.4

Table 3: Coordinates of the observed peaks of $g(r)$.

Peaks	$Q/\sigma[1/\mathring{A}]$			
	NVE/N-H NVT Simulation	MCMC Simulation	Rahman	X-rays
First Peak	1.97	$1,96$	2.0	2.0
Second Peak	3.66	3.66	3.68	3.61
Third Peak	5.41	5.42	5.41	5.41
Fourth Peak	7.20	7.20	7.29	7.17

Table 4: Coordinates of the observed peaks of $S(Q)$.

Now, as in the previous cases, we study the pair correlation function and the structure factor changing some parameters and we compare the results we get with the results provided by the previous simulations to check the consistency. The first parameter we are going to change is the temperature: as we can see we get the same results we previously got with the MD simulations. The same holds changing the density: indeed we can observe that we are getting similar results to the preceding simulations (as in the previous case the calculation of the structure factor isn't stable due to the fact that the integrand has a sinusoidal factor.).

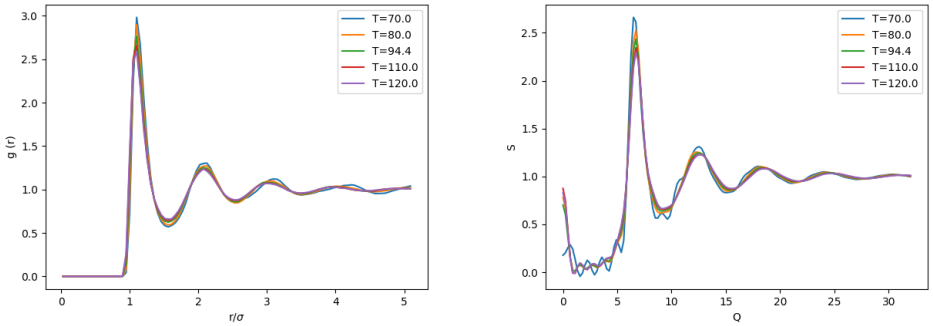

Figure 23: Plot of the pair correlation function (left) and the structure factor (right) obtained during MCMC simulations with different temperatures.

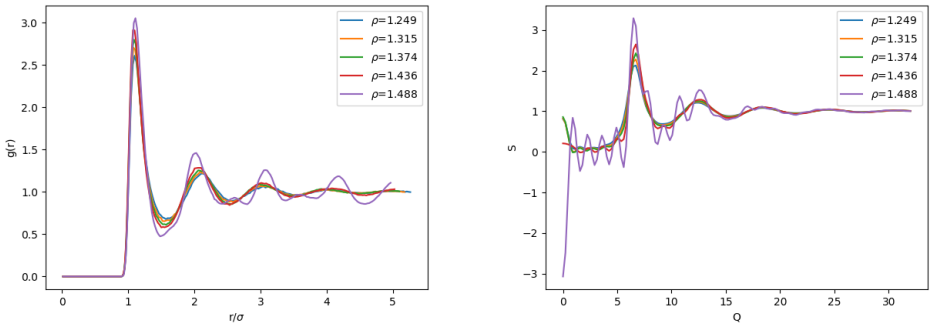

Figure 24: Plot of the pair correlation function (left) and the structure factor (right) obtained during MCMC simulations with different densities.

5 Conclusions

We exploited different techniques to simulate and reproduce the computational experiment of Rahman: throughout all the tests we performed we noticed that MD and MCMC

simulations give comparable results even though, in the second case, we have to build a more complex framework (Markov Chain, time correlation etc..). In the end we can say that if we are working in a framework that deals with an NVE system we will use MD techniques (even though we have to take into account that NVE dynamics has a computational cost that scales as N^2 where N is the number of particles); on the other hand, if we want to simulate a NVT ensemble we can use both the Nosé-Hoover method and the MCMC method: in this case it is important to underline that the first technique has a higher computational complexity and simulations require much more time than the MCMC method. It is important also to underline that the MCMC method is very general and can be adapted to several different situations and it is more computationally efficient (with a comparable accuracy to the other methods) but one has to ensure the convergence of the method before starting to sample.

References

[1] A.Rahman, "Correlations in the Motion of Atoms in Liquid Argon", Physical Review. 136: A405-A411 (1964), https://doi.org/10.1103/PhysRev.136.A405

[2] D. Frenkel, B. Smit, "Understanding Molecular Simulation: from algorithms to applications", ISBN-10: 0122673514